Pseudospectral Technique for Calculation of Atmospheric Boundary Layer Flows

H. N. LEE* AND J. K. SHI**

Department of Meteorology, University of Utah, Salt Lake City, UT 84112

(Manuscript received 17 August 1985, in final form 31 May 1986)

ABSTRACT

A pseudospectral method and its numerical solution algorithm for application to boundary layer problems in the atmosphere are presented. The method introduces the evaluation of a polynomial function when the solution is expressed as the sum of a periodic function and a polynomial function. The periodic function is then treated by Fourier expansion. In the paper, the accuracy of method has been demonstrated. Numerical results for a system of time dependent equations, modeling the atmospheric planetary boundary layer flow and nocturnal flow over terrain are encouraging. The method offers a promising alternative to finite-difference techniques.

1. Introduction

The treatment of the atmospheric Planetary Boundary Layer (PBL) flow is an important part of numerical models of mesoscale or large-scale atmospheric phenomena. Particularly in recent years, efforts have been directed toward prediction in the mesoscale phenomena. To improve the forecast accuracy of boundary layer flow in the predicted mesoscale model has given rise to considerable concern. In this paper, an accurate pseudospectral model for prediction of flow in the PBL is proposed.

In atmospheric models the spectral method and the finite difference method are generally used for discretizing the governing equations. Finite difference methods generally use low-order difference approximations for derivatives and are subject to phase speed errors. Actually, such errors can be minimized or even eliminated by the accurate representation of derivatives through the use of the spectral method (Orszag, 1970, 1971; Machenhauer and Daley, 1974; Gottlieb and Orszag, 1977) or pseudospectral method (Orszag, 1972; Fox and Orszag, 1973; Merilees, 1974; Lee, 1981a, b, 1982). In the pseudospectral method, the governing equations are not actually transformed as they are in the spectral method, rather, the FFT (Fast Fourier Transform) is used to evaluate derivatives in place of finite difference expressions. So far, the spectral or pseudospectral method has been used almost exclusively for large-scale global predictions. No spectral or pseudospectral method has been previously applied successfully to atmospheric boundary layer flow. In this paper, a general pseudospectral numerical algorithm which can be used for simulation of boundary layer flow will be described.

The prediction method using the pseudospectral technique has been developed for the calculation of pollutant transport and diffusion (Lee, 1982, 1986). The technique is promising and encouraging. To increase the capability of the technique, an improved algorithm for easy application of the technique for various problems is further developed here. For the purpose of description of the method and its capability for treating boundaries, particularly the boundaries in the vertical direction, the preliminary calculations of PBL flow are demonstrated.

2. Improved formulations of the pseudospectral technique

In this section, the pseudospectral formulations for calculating values of the spatial derivatives at certain grid points in nonperiodic boundary problems will be presented. They are based on a polynomial subtraction technique (Roach, 1978). This means that one can subtract out the polynomial portion of the solution to form a periodic function. It expresses simply the solution $f(x, t)$ as the sum of a periodic function $f_p(x, t)$ and a polynomial with coefficients b_j in the following form:

$$f(x,t)=f_p(x,t)+b_1(t)x+b_2(t)x^2+b_3(t)x^3+b_4(t)x^4+b_5(t)x^5. \quad (1)$$

The derivatives of $f(x_l, t)$ at each x_l where $l = 1, 2, \cdots, n$ with n grid points are

* Present address: California Research & Technology, Inc., Chatsworth, CA 91311.

** On leave from Department of Meteorology, Lanzhou University, Lanzhou, Gansu, People's Republic of China.

$$\frac{\partial f(x_l,t)}{\partial x}=\frac{\partial f_p(x_l,t)}{\partial x}+b_1(t)+2b_2(t)x_l+3b_3(t)x_l^2+4b_4(t)x_l^3+5b_5(t)x_l^4 \quad (2)$$

$$\frac{\partial^2 f(x_l,t)}{\partial x^2}=\frac{\partial^2 f_p(x_l,t)}{\partial x^2}+2b_2(t)+6b_3(t)x_l+12b_4(t)x_l^2+20b_5(t)x_l^3. \quad (3)$$

The degree of polynomial is of critical importance. Roach (1978) pointed out that first-degree polynomial was completely inadequate. At least degree 3 was required for reasonable accuracy of the first derivative $\partial f/\partial x$ and degree 4 for the second derivative $\partial^2 f/\partial x^2$. The higher degree we applied, the better accuracy we obtained. Thus, degree 5 is used here for demonstration.

In order to calculate $\partial f/\partial x$ and $\partial^2 f/\partial x^2$ in Eqs. (2) and (3), pseudospectral formulations (Lee, 1986) were derived to obtain the values of coefficients $b_j(t)$ satisfying the conditions of periodicity of $f_p(x, t)$ such that

$$f_p{}^{(m)}(x_1,t)=f_p{}^{(m)}(x_n,t); \quad m=0,1,2,3,4 \quad (4)$$

where superscript (m) denoted the mth derivative and the domain of interest was taken to be (x_1, x_n). As indicated in that paper of Lee (1986), the formulations obtained for $m = 1$ and $m = 2$ required the third-order derivatives at boundaries. Actually, those formulations can be constructed in a simple and accurate way without involving high-order derivatives, which are not easy to evaluate. For this reason, a new set of improved formulations will be described and presented. Basically, these sets of formulations are used to solve for the coefficients b_j. Once b_j is evaluated, the values of the derivatives of $\partial f/\partial x$ and $\partial^2 f_p/\partial x^2$ can be evaluated through Fourier expansions at the points x_l $(l = 1, 2, \cdots, n)$.

To derive the formulations, we first write the quintic polynomial spline for a periodic function $f_p(x, t)$ in the last grid interval (x_{n-1}, x_n) instead of last half of interval $(x_{n-1/2}, x_n)$ indicated in the paper of Lee (1986), at time t in the following form

$$f_p(x,t)=\alpha_1(x-x_{n-1})^5+\alpha_2(x-x_{n-1})^4+\alpha_3(x-x_{n-1})^3+\alpha_4(x-x_{n-1})^2+\alpha_5(x-x_{n-1})+\alpha_6. \quad (5)$$

For the simplicity of notations, the $f^{(m)}_{p,x_{n-1}}$, $f^{(m)}_{p,x_2}$ and $f^{(m)}_{p,x_n}$ are used to denote $f_p{}^{(m)}(x_{n-1}, t)$, $f_p{}^{(m)}(x_2, t)$ and $f_p{}^{(m)}(x_n, t)$, respectively, in the following derivations. By differentiating Eq. (5) at $x = x_n$ and $x = x_{n-1}$, one can construct the following system of linear algebraic equations in α_1, α_2 and α_3:

$$\alpha_1 h^5+\alpha_2 h^4+\alpha_3 h^3=f_{p,x_n}-f_{p,x_{n-1}}-hf^{(1)}_{p,x_{n-1}}-\frac{h^2}{2}f^{(2)}_{p,x_{n-1}} \quad (6)$$

$$5\alpha_1 h^4+4\alpha_2 h^3+3\alpha_3 h^2=f^{(1)}_{p,x_n}-f^{(1)}_{p,x_{n-1}}-hf^{(2)}_{p,x_{n-1}} \quad (7)$$

$$20\alpha_1 h^3+12\alpha_2 h^2+6\alpha_3 h=f^{(2)}_{p,x_n}-f^{(2)}_{p,x_{n-1}} \quad (8)$$

where $h = x_n - x_{n-1}$ is a grid interval.

By solving Eqs. (6), (7) and (8), one obtains

$$\alpha_1=-(f^{(2)}_{p,x_{n-1}}-f^{(2)}_{p,x_n})/2h^3-3(f^{(1)}_{p,x_{n-1}}+f^{(1)}_{p,x_n})/h^4-6(f_{p,x_{n-1}}-f_{p,x_n})/h^5 \quad (9)$$

$$\alpha_2=(3f^{(2)}_{p,x_{n-1}}-2f^{(2)}_{p,x_n})/2h^2+(8f^{(1)}_{p,x_{n-1}}+7f^{(1)}_{p,x_n})/h^3+15(f_{p,x_{n-1}}-f_{p,x_n})/h^4 \quad (10)$$

$$\alpha_3=-(3f^{(2)}_{p,x_{n-1}}-f^{(2)}_{p,x_n})/2h-2(3f^{(1)}_{p,x_{n-1}}+2f^{(1)}_{p,x_n})/h^2-10(f_{p,x_{n-1}}-f_{p,x_n})/h^3. \quad (11)$$

The values of α_4, α_5 and α_6 are, respectively, $0.5f^{(2)}_{p,x_{n-1}}$, $f^{(1)}_{p,x_{n-1}}$ and $f_{p,x_{n-1}}$. Similarly, in the first grid interval from x_1 to x_2, one can write the polynomial spline for the periodic function $f_p(x, t)$ at time t as

$$f_p(x,t)=\beta_1(x-x_1)^5+\beta_2(x-x_1)^4+\beta_3(x-x_1)^3+\beta_4(x-x_1)^2+\beta_5(x-x_1)+\beta_6. \quad (12)$$

With the same manner as before, we can have the solutions of β_1, β_2, β_3, β_4, β_5 and β_6 in terms of the values of periodic function and its first and second derivatives at the points $x = x_1$ and $x = x_2$.

Then, taking the fourth derivatives in (5) and (12) and using (4) with $m = 4$, we have

$$24\beta_2=120\alpha_1 h+24\alpha_2. \quad (13)$$

Substituting the values of β_2, α_2 obtained previously into the above equation, we simply get the relationship

$$f^{(2)}_{p,x_{n-1}}-f^{(2)}_{p,x_2}+\frac{1}{h}(7f^{(1)}_{p,x_{n-1}}+16f^{(1)}_{p,x_n}+7f^{(1)}_{p,x_2})+\frac{15}{h^2}(f_{p,x_{n-1}}-f_{p,x_2})=0. \quad (14)$$

Similarly, to satisfy $m = 3$ in Eq. (4), we obtain another relationship

$$f^{(2)}_{p,x_{n-1}}-6f^{(2)}_{p,x_n}+f^{(2)}_{p,x_2}+\frac{8}{h}(f^{(1)}_{p,x_{n-1}}-f^{(1)}_{p,x_2})+\frac{20}{h^2}(f_{p,x_{n-1}}-2f_{p,x_n}+f_{p,x_2})=0. \quad (15)$$

Similar formulae for $m = 1$ and $m = 2$ can be obtained. The corresponding formulae shown in Lee (1986) are complicated and involve third-order derivatives which need to be evaluated. To avoid the third-order derivatives in the present approach, we take the second-derivative in (5) and evaluate it at $x = x_{n-1/2}$ with the use of the values of α_1, α_2, α_3 and α_4 obtained earlier. After some algebra arrangement and using the central difference for $f^{(2)}_{p,x_{n-1/2}}$ we have

$$f^{(2)}_{p,x_n}=-f^{(2)}_{p,x_{n-1}}-\frac{2}{h}f^{(1)}_{p,x_{n-1}}+\frac{2}{h}f^{(1)}_{p,x_n}. \quad (16)$$

Similarly, one can obtain from Eq. (12) by taking the second derivative at $x = x_{1.5}$

$$f^{(2)}_{p,x_1} = -f^{(2)}_{p,x_2} - \frac{2}{h} f^{(1)}_{p,x_n} + \frac{2}{h} f^{(1)}_{p,x_2}. \quad (17)$$

Equating Eq. (16) to Eq. (17) by using Eq. (4) for $m = 2$, we obtain the following relationship

$$f^{(2)}_{p,x_{n-1}} - f^{(2)}_{p,x_2} + \frac{2}{h}(f^{(1)}_{p,x_{n-1}} - 2f^{(1)}_{p,x_n} + f^{(1)}_{p,x_2}) = 0. \quad (18)$$

Consequently, to have relationship for $m = 1$, the same procedure as the one for $m = 2$ is used. We differentiate Eqs. (5) and (12) to obtain their first derivatives and evaluate them at $x = x_{n-1/2}$ and $x = x_{1.5}$, respectively. We finally have

$$f^{(2)}_{p,x_{n-1}} - 2f^{(2)}_{p,x_n} + f^{(2)}_{p,x_2} + \frac{14}{h}(f^{(1)}_{p,x_{n-1}} - f^{(1)}_{p,x_2}) + \frac{28}{h^2}(f_{p,x_{n-1}} - 2f_{p,x_n} + f_{p,x_2}) = 0. \quad (19)$$

Hence, Eqs. (14), (15), (18) and (19) form a new set of formulations that will be used later for calculating the coefficients $b_j(t)$ of the polynomial in Eq. (1). In Eqs. (14), (15), (18) and (19), $f_{p,x_{n-1}}, f_{p,x_n}, f_{p,x_2}$ and their derivatives can be expressed by Fourier expressions to have the following forms (Lee, 1986).

$$f_{p,x_i} = \sum_{l=1}^{n} \left\{ \frac{1}{n} \sum_{K} \cos[K(x_i - x_l)] \right\} \left\{ f(x_l, t) - \sum_{j=1}^{5} b_j x_l^{\,j} \right\} \quad (20)$$

$$f^{(1)}_{p,x_i} = \sum_{l=1}^{n} \left\{ \frac{1}{n} \sum_{K} -K \sin[K(x_i - x_l)] \right\} \left\{ f(x_l, t) - \sum_{j=1}^{5} b_j x_l^{\,j} \right\} \quad (21)$$

$$f^{(2)}_{p,x_i} = \sum_{l=1}^{n} \left\{ \frac{1}{n} \sum_{K} -K^2 \cos[K(x_i - x_l)] \right\} \times \left\{ f(x_l, t) - \sum_{j=1}^{5} b_j x_l^{\,j} \right\}. \quad (22)$$

If the boundary values for $f(x, t)$ are specified or given from the values obtained at the previous time step, an additional relationship for b_j satisfying $f_p(x_1, t) = f_p(x_n, t)$ of Eq. (4) is

$$\sum_{j=1}^{5} b_j(x_n^{\,j} - x_1^{\,j}) = f(x_n, t) - f(x_1, t). \quad (23)$$

Hence, there are five equations for five unknowns b_j ($j = 1, 2, \cdots, 5$). The values of b_j can be easily obtained by solving 5×5 matrix. The derivatives $\partial f/\partial x$ and $\partial^2 f/\partial x^2$ are then easily evaluated from Eqs. (2) and (3) in which the derivatives of periodic function are the forms of Eqs. (21) and (22).

3. Accuracy tests

In order to test the accuracy of the pseudospectral technique described herein for evaluating the spatial derivatives, we use two analytical functions on a one-dimensional grid for demonstration. These functions are nonperiodic.

For the first example, we use an exponential function $f = e^x$ that give rise to a "ringing" or Gibbs phenomena at the boundaries in the finite Fourier expansion which greatly slows the convergence. To reduce or minimize the "ringing" in the finite Fourier expansion, we use Eq. (1) by subtracting the polynomial from the solution. The coefficients b_j ($j = 1, 2, \cdots, 5$) of polynomial are computed by using Eqs. (14), (15), (18), (19) and (23). The derivatives of $\partial f_p/\partial x$ and $\partial^2 f_p/\partial x^2$ are then computed with using b_1, b_2, b_3, b_4 and b_5, and finally $f^{(1)} = \partial f/\partial x$ and $f^{(2)} = \partial^2 f/\partial x^2$ are evaluated. The results are compared with the analytical values by evaluating the local relative errors which are defined as $(f^{(1)}_{\text{analytical}} - f^{(1)}_{\text{numerical}})/f^{(1)}_{\text{analytical}}$ for the first derivative of function f and $(f^{(2)}_{\text{analytical}} - f^{(2)}_{\text{numerical}})/f^{(2)}_{\text{analytical}}$ for the second derivative. The technique produces very accurate first and second derivatives, as seen in Fig. 1. The accuracy is improved by increasing the number of grid points. The local relative errors for $f^{(1)}$ are smaller than those for $f^{(2)}$.

For the second example, the damped sine wave (Roach, 1978) as shown in Fig. 2a is selected here with $a = -2$ and $b = 3/4$. The comparisons of exact with the computed first and second derivative located on a grid of 32 points are shown in Fig. 2b. The excellent accuracy in Fig. 2b further indicates that the polynomial evaluations in the present pseudospectral technique for nonperiodic problems are encouraging.

4. Simulation of atmospheric boundary layer flow

For problems involving vertical coordinates in the PBL, a finite difference or finite element method is generally used for vertical difference approximations. Since the pseudospectral technique presented here yields higher-order accuracy for computing derivatives, we apply it to the following one-dimensional time-dependent PBL model equation in the z-direction

$$\frac{\partial U}{\partial t} = f_c(V - V_g) + \frac{\partial}{\partial z}\left(K_m \frac{\partial U}{\partial z}\right) \quad (24)$$

$$\frac{\partial V}{\partial t} = -f_c(U - U_g) + \frac{\partial}{\partial z}\left(K_m \frac{\partial V}{\partial z}\right) \quad (25)$$

with the boundary conditions

$$U(0, t) = V(0, t) = 0 \quad \text{at} \quad z = 0 \quad (26)$$

$$U(H, t) = U_g, \quad V(H, t) = V_g \quad \text{at} \quad z = H \quad (27)$$

where (U, V), (U_g, V_g), f_c, K_m and H are velocities,

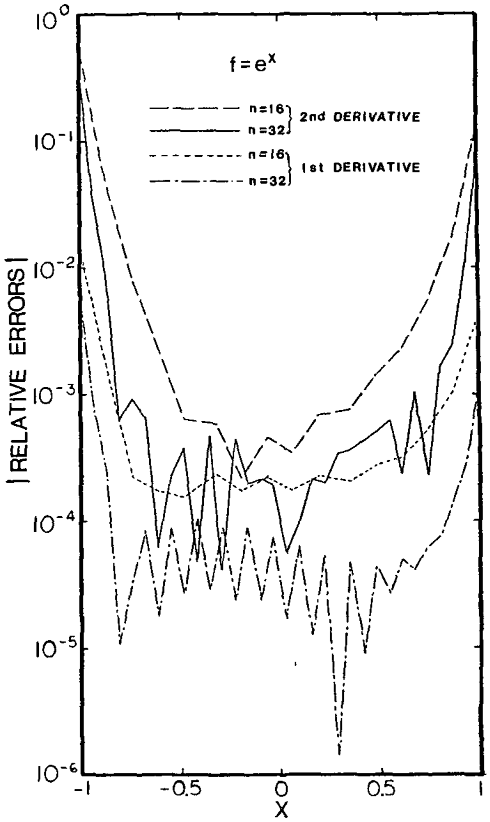

FIG. 1. Local relative errors of computed derivatives of an exponential function on a discrete grid with grid points $n = 16$ and $n = 32$.

geostrophic winds, Coriolis force parameter, eddy diffusivity and height of PBL, respectively.

In the first case, the constant eddy diffusivity K_m is assumed. Based on Eqs. (1), (2) and (3), the Eqs. (24) and (25) using a backward time difference scheme can be written in the following form

$$U_p''^{[n+1]} - \frac{1}{\Delta t K_m} U_p^{[n+1]} + \frac{f_c}{K_m} V_p^{[n+1]} = \frac{f_c}{K_m} V_g + \frac{1}{\Delta t K_m} \sum_{j=1}^{5} a_j^{[n+1]} z^j - \frac{f_c}{K_m} \sum_{j=1}^{5} b_j^{[n+1]} z^j - \sum_{j=1}^{5} j(j-1) a_j^{[n+1]} z^{j-2} - \frac{1}{\Delta t K_m} U^{[n]} \quad (28)$$

$$V_p''^{[n+1]} - \frac{1}{\Delta t K_m} V_p^{[n+1]} - \frac{f_c}{K_m} U_p^{[n+1]} = -\frac{f_c}{K_m} U_g + \frac{1}{\Delta t K_m} \sum_{j=1}^{5} b_j^{[n+1]} z^j + \frac{f_c}{K_m} \sum_{j=1}^{5} a_j^{[n+1]} z^j - \sum_{j=1}^{5} j(j-1) b_j^{[n+1]} z^{j-2} - \frac{1}{\Delta t K_m} V^{[n]} \quad (29)$$

where Δt is a time step, $U_p^{[n+1]}$ and $V_p^{[n+1]}$ is a periodic function at time $[n+1]\Delta t$ in U- and V-component, respectively. $U_p''^{[n+1]}$ and $V_p''^{[n+1]}$ stands for $\partial^2 U_p^{[n+1]}/\partial z^2$ and $\partial^2 V_p^{[n+1]}/\partial z^2$, respectively. Here $u^{[n]}$ and $V^{[n]}$ stands for the value at previous time step for the U- and V-component, respectively, and $a_j^{[n+1]}$ and $b_j^{[n+1]}$ are polynomial coefficients at time $[n+1]\Delta t$ for the U- and V-component, respectively.

Since U_p and V_p are real values, their derivatives have the following form

$$U''_{p,z_i} = \sum_{l=1}^{n} C(z_i, z_l) U_p, z_l \quad (30)$$

$$V''_{p,z_i} = \sum_{l=1}^{n} C(z_i, z_l) V_p, z_l \quad (31)$$

in which

$$C(z_i, z_l) = \left\{ \frac{1}{n} \sum_{K} -K^2 \cos[K(z_i - z_l)] \right\} \quad (32)$$

where $i = 1, 2, \cdots, n$ and $z_i = (i-1)\Delta z$, which Δz is a grid interval in the vertical direction and $z_n = H$.

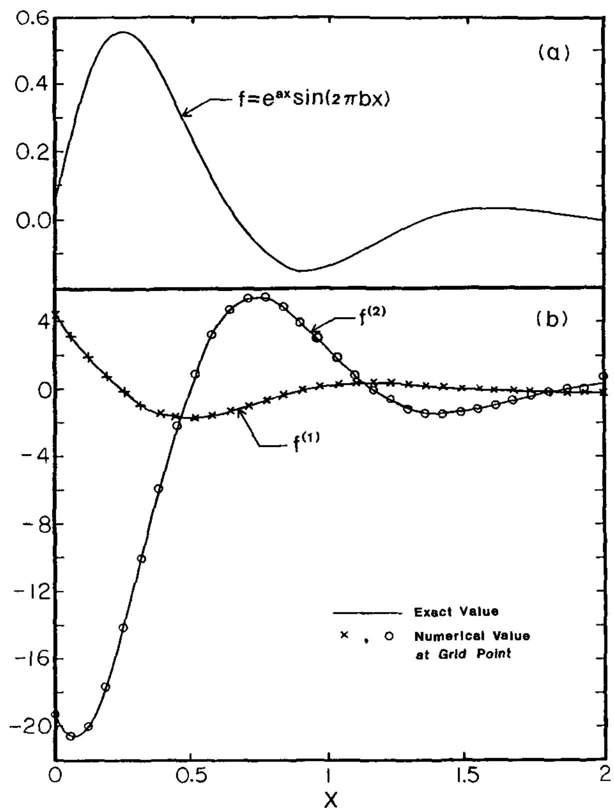

FIG. 2. Computed derivatives (b) of a damped sine wave (a) on a grid of 32 points.

From boundary conditions of Eqs. (26) and (27) we have

$$U_{p,z_1} = U(0, t)$$

$$V_{p,z_1} = V(0, t)$$

$$U_{p,z_n} = U_g - \sum_{j=1}^{5} a_j z_n{}^j$$

$$V_{p,z_n} = V_g - \sum_{j=1}^{5} b_j z_n{}^j. \tag{33}$$

With the use of Eqs. (30), (31) and (33), Eqs. (28) and (29) are combined in a matrix form

$$[C]\{A_p\} = \{B\} \tag{34}$$

where the square bracket represents a square matrix and the braces represent a column vector. Matrix $[C]$ contains the values of $C(z_i, z_l)$ from Eq. (32) and the values of $-1/K_m\Delta t$ and f_c/K_m from the left-hand side of Eqs. (28) and (29); $\{A_p\}$ is the column vector of $(U_{p,z_1}, U_{p,z_2}, \ldots, U_{p,z_n}, V_{p,z_1}, V_{p,z_2}, \ldots, V_{p,z_n})$. Vector $\{B\}$ is formed by the values of the right-hand side of Eqs. (28) and (29).

The coefficients a_j and b_j are obtained by solving Eqs. (14), (15), (18), (19) and (23). Equation (34) is solved iteratively at each time step by the Gauss-Seidel method using the last grid values of U_p and V_p to update $\{B\}$. Based on the computed values of U_p and V_p, U and V are finally obtained

$$\left.\begin{aligned} U^{[n+1]}(z_l, t) &= U_{p,z_l}^{[n+1]} + \sum_{j=1}^{5} a_j{}^{[n+1]} z_l{}^j \\ V^{[n+1]}(z_l, t) &= V_{p,z_l}^{[n+1]} + \sum_{j=1}^{5} b_j{}^{[n+1]} z_l{}^j \end{aligned}\right\}, l = 1, 2, \cdots, n. \tag{35}$$

The process is then repeated until steady state occurs. The numerical results for K_m = 10 m^2 s^{-1} in Table 1, which are steady state solutions, are compared with the Ekman analytical solution (Ekman, 1905) of Eqs. (24) and (25). In Table 1, U_g = 5 m s^{-1} and V_g = 1 m s^{-1} are used. It is seen that the numerical solutions using the present pseudospectral technique agree very well with the analytical solutions. The discrepancies between the numerical and analytical solutions can be significantly reduced when a smaller mesh spacing is used. This example shows that, in order to override the periodic boundary conditions, the technique of introducing the polynomial into solution works successfully in the simulation of the boundary layer flow. As a second case, a linear variation of eddy diffusivity with height is assumed. It takes the following form

$$K_m = \lambda_1 z + \lambda_2 \tag{36}$$

where λ_1 and λ_2 are prescribed values in unit m s^{-1}. Hence, Eqs. (24) and (25) contain first derivatives which

TABLE 1. Comparison of the Ekman analytical solution with numerical results for constant vertical eddy diffusivity by assuming U_g = 5 m s^{-1} and V_g = 1 m s^{-1}.

		U-Component (m s^{-1})		V-Component (m s^{-1})	
Grid	Height (m)	Analytical	Numerical	Analytical	Numerical
1	0.0	0.000	−0.000	0.000	−0.000
2	99.5	0.920	0.889	1.103	0.954
3	199.1	1.833	1.784	1.801	1.718
4	298.6	2.669	2.612	2.185	2.128
5	398.1	3.389	3.331	2.337	2.313
6	497.7	3.979	3.922	2.329	2.325
7	597.2	4.437	4.384	2.218	2.230
8	696.7	4.776	4.726	2.050	2.071
9	796.3	5.011	4.964	1.859	1.882
10	895.8	5.160	5.115	1.669	1.689
11	995.3	5.243	5.199	1.494	1.503
12	1094.9	5.277	5.234	1.343	1.338
13	1194.4	5.277	5.237	1.219	1.189
14	1293.9	5.255	5.222	1.122	1.074
15	1393.5	5.220	5.200	1.050	0.954
16	1493.0	5.181	5.181	1.000	1.000

are added to the previous test that involves only second derivatives. By using Eq. (36), the steady-state analytical solutions (Yeh, 1983) to Eqs. (24) and (25) are

$$U = c_1 \operatorname{Ber}(\eta) - c_2 \operatorname{Bei}(\eta) + c_3 \operatorname{Ker}(\eta) - c_4 \operatorname{Kei}(\eta) + U_g \tag{37}$$

$$V = c_1 \operatorname{Bei}(\eta) + c_2 \operatorname{Ber}(\eta) + c_3 \operatorname{Kei}(\eta) + c_4 \operatorname{Ker}(\eta) + V_g \tag{38}$$

where $\eta = 2(f_c K_m)^{1/2}/\lambda_1$. Ber and Bei are Bessel functions. Ker and Kei are Kelvin functions (Abramowitz and Stegun, 1969). The constants c_i can be determined from the boundary conditions Eqs. (26)–(27).

The numerical procedures for this case are the same as the first case. The final steady-state numerical results for λ_1 = 0.1 m s^{-1} and λ_2 = 10 m s^{-1} are compared with the analytical solutions of Eqs. (37) and (38). The comparisons are shown in Table 2 for U_g = 5 m s^{-1}, V_g = 1 m s^{-1}. It is seen from Table 2 that the pseudospectral technique proposed here also works very well for the solution of boundary layer flow with consideration of height change of eddy diffusivity.

The next example uses the pseudospectral technique to test the nocturnal boundary layer flow over terrain with slope angle δ. The governing equations may be written (Rao and Snodgrass, 1981)

$$\frac{\partial u'}{\partial t} = f_c v' + \frac{\partial}{\partial z^*}\left(K_m \frac{\partial u'}{\partial z^*}\right) - (g/\theta_0)\theta' \sin\delta \tag{39}$$

$$\frac{\partial v'}{\partial t} = f_c u' + \frac{\partial}{\partial z^*}\left(K_m \frac{\partial v'}{\partial z^*}\right) \tag{40}$$

$$\frac{\partial \theta'}{\partial t} = u'\gamma \sin\delta + \frac{\partial}{\partial z^*}\left(K_h \frac{\partial \theta'}{\partial z^*}\right) \tag{41}$$

TABLE 2. As in Table 1 except for linear variation of vertical eddy diffusivity with height.

Grid	Height (m)	U-Component ($m s^{-1}$)		V-Component ($m s^{-1}$)	
		Analytical	Numerical	Analytical	Numerical
1	0.0	0.000	−0.000	0.000	−0.000
2	99.5	1.300	1.247	0.836	0.746
3	199.1	2.071	2.015	1.170	1.098
4	298.6	2.614	2.558	1.322	1.252
5	398.1	3.029	2.974	1.385	1.319
6	497.7	3.360	3.308	1.402	1.336
7	597.2	3.635	3.586	1.390	1.324
8	696.7	3.867	3.822	1.361	1.295
9	796.3	4.068	4.027	1.323	1.255
10	895.8	4.245	4.208	1.279	1.209
11	995.3	4.401	4.370	1.231	1.159
12	1094.9	4.543	4.517	1.183	1.109
13	1194.4	4.671	4.651	1.135	1.057
14	1293.9	4.789	4.775	1.088	1.012
15	1393.5	4.898	4.890	1.043	0.954
16	1493.0	5.000	5.000	1.000	1.000

where $u' = U - U_g$, $v' = V - V_g$ and $\theta' = \theta - \theta_0$ is the deviation of the mean potential temperature from an undisturbed reference state atmospheric distribution $\theta_0(z)$, defined such that $\partial\theta_0/\partial z = \gamma =$ constant > 0; g is the acceleration due to gravity and z^* is a normal axis to the terrain surface.

At $z^* = 0$, the lower boundary conditions are

$$u' = -U_g, \quad v' = -V_g, \quad \theta' = -\Delta_0 \tag{42}$$

where Δ_0 is the magnitude of the surface cooling. At $z^* = H$ the upper boundary conditions are

$$u' = v' = \theta' = 0. \tag{43}$$

Steady-state analytical solutions for Eqs. (39)–(41) obtained by assuming $K_m = K_h$ to be constants in the boundary layer, were given by Lykosov and Gutman (1972). To compare numerical solutions with analytical solutions the flow parameters $\delta = 10°$, $\Delta_0 = 4°C$, $\gamma = 0.004°C\ m^{-1}$, $f_c \approx 10^{-4}\ s^{-1}$, $g/\theta_0 = 0.0033\ m\ s^{-2}\ k^{-1}$ and $K_m = K_h = 100\ m^2\ s^{-1}$ were used. The comparisons between the steady-state numerical solutions and analytical solutions are shown in Table 3 for $U_g = 5\ m\ s^{-1}$, $V_g = -0.576\ m\ s^{-1}$ and in Table 4 for $U_g = 0\ m\ s^{-1}$, $V_g = -0.576\ m\ s^{-1}$. The agreement between the numerical and analytical solutions is excellent. This example further confirms the feasibility and applicability of the pseudospectral technique for simulation of atmospheric boundary layer flow.

5. Conclusions and discussions

A numerical solution algorithm has been derived, employing pseudospectral theory, for simulation of atmospheric boundary layer flow. The technique is to express the boundary layer solution as the sum of periodic and polynomial parts. This technique involves the evaluation of a polynomial function at each time step. The Fourier expansions are applied to the periodic function. The accuracy has been demonstrated in the paper. From comparing solutions of the advection equation by using the present technique with results using other numerical techniques, it is found (Lee, 1986) that the solutions based on the present technique give much better agreement with the analytical solution. For the simulation of atmospheric boundary layer flow, the pseudospectral technique described here offers a promising alternative to finite-difference methods,

TABLE 3. Comparison of analytical solution with numerical results for nocturnal boundary layer flow over terrain by assuming $U_g = 5\ m\ s^{-1}$ and $V_g = -0.576\ m\ s^{-1}$.

Grid	Height (m)	U-Component ($m s^{-1}$)		V-Component ($m s^{-1}$)		Potential temperature	
		Analytical	Numerical	Analytical	Numerical	Analytical	Numerical
1	0.0	0.000	0.000	0.000	0.000	−4.000	−4.000
2	93.7	3.939	3.964	−0.112	−0.108	−3.223	−3.252
3	187.3	6.256	6.289	−0.234	−0.233	−2.373	−2.386
4	281.0	7.374	7.407	−0.346	−0.346	−1.593	−1.602
5	374.7	7.683	7.712	−0.438	−0.439	−0.954	−0.956
6	468.3	7.505	7.529	−0.507	−0.508	−0.477	−0.475
7	562.0	7.079	7.100	−0.554	−0.556	−0.150	−0.145
8	655.7	6.573	6.592	−0.583	−0.585	0.050	0.056
9	749.3	6.088	6.108	−0.598	−0.600	0.154	0.160
10	843.0	5.678	5.702	−0.603	−0.606	0.192	0.196
11	936.7	5.362	5.393	−0.603	−0.605	0.188	0.189
12	1030.3	5.141	5.179	−0.599	−0.601	0.161	0.158
13	1124.0	5.000	5.043	−0.594	−0.596	0.125	0.114
14	1217.7	4.922	4.965	−0.589	−0.590	0.089	0.071
15	1311.3	4.889	4.923	−0.584	−0.584	0.057	0.020
16	1405.0	4.885	4.885	−0.581	−0.581	0.032	0.032

TABLE 4. As in Table 3 except for $U_g = 0$ m s^{-1} and $V_g = -0.576$ m s^{-1}.

Grid	Height (m)	U-Component (m s^{-1})		V-Component (m s^{-1})		Potential temperature	
		Analytical	Numerical	Analytical	Numerical	Analytical	Numerical
1	0.0	0.000	0.000	0.000	0.000	−4.000	−4.000
2	93.7	2.496	2.559	−0.166	−0.153	−2.846	−2.932
3	187.3	3.551	3.640	−0.312	−0.305	−1.836	−1.879
4	281.0	3.672	3.763	−0.426	−0.422	−1.038	−1.065
5	374.7	3.260	3.340	−0.509	−0.508	−0.462	−0.469
6	468.3	2.608	2.672	−0.564	−0.564	−0.082	−0.080
7	562.0	1.907	1.956	−0.596	−0.597	0.138	0.149
8	655.7	1.270	1.311	−0.611	−0.613	0.242	0.258
9	749.3	0.753	0.793	−0.614	−0.617	0.268	0.286
10	843.0	0.368	0.416	−0.612	−0.614	0.247	0.265
11	936.7	0.108	0.173	−0.605	−0.608	0.204	0.218
12	1030.3	0.000	0.038	−0.598	−0.600	0.153	0.161
13	1124.0	0.000	−0.015	−0.591	−0.592	0.105	0.098
14	1217.7	0.000	−0.018	−0.585	−0.584	0.065	0.043
15	1311.3	0.000	−0.001	−0.581	−0.575	0.034	−0.031
16	1405.0	0.000	−0.000	−0.578	−0.578	0.013	0.013

which are generally used in the vertical direction for boundary layer problems. It has been shown in Yeh (1983) for a similar boundary layer problem that the simple finite element method required more grids (i.e., finer zoning) to reach the same accuracy as the method presented here. This is because a high degree polynomial is used in our method. When the degree of polynomial is higher, the coefficients in the Fourier series decrease quicker. Thus, the rate of convergence of the Fourier series is faster in this situation, and a small number of terms provide a rather good approximation. When the pseudospectral interpolation is used to approximate space derivatives, this means that good results could be expected even if a smaller number of grid points is used. This is true when the representation of the original function as a sum of a periodic function and a polynomial could be performed exactly. In practice, this cannot be done due to the limitations of polynomials to a certain degree. To minimize the rounding errors, high degree polynomials are required and hence, performed in the present paper. Future studies will be conducted on the boundness of these errors and convergence of the technique for various classes of problems.

REFERENCES

Abramowitz, M., and I. A. Stegan, 1969: *Handbook of Mathematical Functions,* Dover, 379–384.

Ekman, V. W., 1905: On the influence of the earth's rotation on ocean-currents. *Ark. Mat. Astron. Fys.,* **11,** 1–52.

Fox, D. G., and S. A. Orszag, 1973: Pseudospectral approximation to two-dimensional turbulence. *J. Comput. Phys.,* **11,** 612–619.

Gottlieb, D., and S. A. Orszag, 1977: *Numerical Analysis of Spectral Methods: Theory and Applications. NSF-CBMS Monogr.* No. 26, SIAM.

Lee, H. N., 1981a: An alternate pseudospectral model for pollutant transport, diffusion and deposition in the atmosphere. *Atmos. Environ.,* **15,** 1017–1024.

——, 1981b: Pseudospectral method for problems with nonperiodic boundary conditions. *Symp. of Numerical Boundary Condition Procedures,* California, NASA Ames Research Center, 313–322.

——, 1982: Numerical model of pollutant transport and dispersion using pseudospectral method. *Third Joint Conf. on Applications of Air Pollution Meteorology,* San Antonio, Sponsor, xx pp.

——, 1986: On a pseudospectral method for advection-diffusion equations of an atmospheric pollutant. *Int. J. Environ. Stud.* (in press).

Lykosov, V. N., and L. N. Gutman, 1972: Turbulent boundary layer above a sloping underlying surface. *Izv. Atmos. Oceanic Phys.,* **8,** 462–467.

Machenhauer, B., and R. Daley, 1974: Hemispheric spectral model. GARP Publ. Ser. No. 14, 226–251.

Merilees, P. E., 1974: Numerical experiments with the pseudospectral method in spherical coordinates. *Atmosphere,* **12,** 77–96.

Orszag, S. A., 1970: Transform method for calculation of vector-coupled sums: Application to the spectral form of the vorticity equation. *J. Atmos. Sci.,* **27,** 890–895.

——, 1971: Numerical simulations of incompressible flows within simple boundaries: Accuracy. *J. Fluid Mech.,* **49,** 75–112.

——, 1972: Comparison of pseudospectral and spectral approximations. *Stud. Appl. Math,* **51,** 253–259.

Rao, K. S., and H. F. Snodgrass, 1981: The nocturnal boundary layer over a sloping surface. *Fifth Symp. on Turbulence, Diffusion and Air Pollution,* Atlanta, Amer. Meteor. Soc., 106–108.

Roach, P. J., 1978: A pseudospectral FFT technique for non-periodic problems. *J. Comput. Phys.,* **27,** 204–220.

Yeh, E. N., 1983: Prediction of atmospheric flow and dispersion over sloping terrain. Ph.D. thesis, University of Utah, 166 pp.